George Sony (Orcid ID: 0000-0002-9848-0465)

Folic acid incorporated Nitrogen-doped Carbon dots as a turn-on fluorescence probe for homocysteine detection.

Anju S Madanan [a], Aswathy A.O. [a], Susan Varghese[a], Merin K. Abraham [a], Lekshmi R.S. [a], Ali Ibrahim Shkhair[a], Lekha G.M. [a], Syamchand S, S [b], and Sony George [a]

Corresponding Author

Dr. Sony George

Associate Professor,

[a] Department of Chemistry, School of Physical and Mathematical Science, University of Kerala, Thiruvananthapuram, Kerala, India- 695581 Mob: +919446462933

Email: emailtosony@gmail.com

[a] Department of Chemistry, School of Physical and Mathematical Science, University of Kerala, Thiruvananthapuram, Kerala, India- 695581

[b] Department of Chemistry, University College, Thiruvananthapuram, Kerala, India- 695034

Abstract

This study describes the development of a low-cost fluorescence assay for detecting homocysteine (Hcy) without the interference of cysteine and glutathione using carbon quantum dots. Herein nitrogen-doped carbon quantum dots (NCD) were synthesized from citric acid as the carbon source and urea as the dopant using a one-pot microwave-assisted

This article has been accepted for publication and undergone full peer review but has not been through the copyediting, typesetting, pagination and proofreading process which may lead to differences between this version and the Version of Record. Please cite this article as doi: 10.1002/bio.4411

method. The obtained NCDs were incorporated with folic acid (FA) by the direct ex-situ addition method and were used as a fluorescence probe to detect Hcy. The probe exhibited a fluorescence turn-on response with increased Hcy concentration up to 50 µM with a limit of detection of 2.276 µM. The point of care detection of Hcy using the probe was also tested with a paper-based assay strip.

Keywords

Bio thiols, biosensor, homocysteine, inflammation, biomarker, cysteine, paper strip assay

1. Introduction.

Cardiovascular diseases (CVD) are a universal concern as it accounts for three quadrants of premature death and disability globally[1]. The long-term persistence of CVD abides the patient and his near ones into economic and emotional havoc[2]. The tight and stressful life schedule and the unhealthy food habits of this era accelerate CVD development at early productive ages of the last thirty's or first forty's, which adversely affects the national human resources. Hence timely detection at the earliest and appropriate monitoring is vital in effectively managing CVD. Inflammation and atherosclerosis are observed as the prime phase of CVD development. Inflammation is the initial signature of the onset of cardiovascular disease, so its recognition and appraisal are crucial in the early detection of CVD. Therefore, the early assessment of the onset of inflammation helps clinicians in reducing the death and disability rate due to the development of chronic CVD. Assessment of biomarkers is the most powerful tool in diagnosing and prognosing diseases. Many biomarkers are identified and assessed to diagnose and prognosis different CVD stages.

Homocysteine (Hcy) is a Sulphur containing amino acid and a molecule of high clinical significance as an independent prognostic marker of different diseases, including CVD, Alzheimer's, etc. It was well established that the elevated homocysteine (Hcy) levels in our body are a premonition factor for CVD and Alzheimer's disease. Hcy (2-amino-4-mercapturic acid) takes part in cellular homeostasis with multiple roles such as a cyto

protectant, a messenger inhibiting insulin, and an anti-inflammation agent[3,4]. Hcy is intricate in pro-atherosclerosis by instigating oxidative stress and methylation modification. In humans, the synthesized Hcy usually gets converted to methionine and cysteine, and the average level of Hcy in the plasma of healthy persons lies in the range of about 6.7 to 14.5 μM[5–7]. The concentration of Hcy in plasma above 15 μM is known as hyperhomocysteinemia, with > 100 μM regarded as severe, 30 -100 μM as intermediate, and 15-30 μM moderate[5–8]. Homocystinuria is a genetic disorder, and high amounts of Hcy are noxious to the extracellular matrix and endothelial tissues, leading to clotting and thrombogenesis [9–12]. Several clinical studies assessed the effect of high concentration at different stages of CVD disease ranging from atherosclerosis to stroke or myocardial infarction[11–14].

The traditional methods of Hcy detection include chromatographic techniques like GC, HPLC, capillary electrophoresis, etc., which are tedious, expensive, and confined to centralized laboratories[6]. Another major challenge during the detection of Hcy is the interference caused by its sister homologue cysteine, which differs only by a single methylene group[7]. This situation points towards the need for new methods for the onsite rapid and low-cost detection of Hcy. Optical methods, especially fluorescence-based detection methods, possess several merits, including low cost, simplicity, good selectivity, sensitivity, ease of handling, and real-time detection[6,15]. The sensing with fluorescence probes developed from nanostructures is the better candidate for creating highly efficient, cost-effective diagnostics[16,17]. Owing to the advantages like ease of preparation, availability of precursors, better biocompatibility, and better quantum yields, Carbon quantum dots or carbon dots are considered an excellent fluorescent nanoprobe[18,19]. Hetro atom-doped carbon dots are preferred for their excellent optical properties over virgin C-dots[16].

We were inspired by certain recent studies on selective detection of Hcy using a different substrate such as fluorescein tri aldehyde[20], Nitrogen-doped graphene quantum dots, etc.[21]. We attempted the development of folic acid-incorporated nitrogen-doped carbon quantum dots (FA-NCDs) for the selective fluorescence detection of Hcy. The nitrogen-doped carbon dots (NCD) were prepared by using microwave-assisted synthesis and conjugated with folic acid by ex-situ addition. The ex-situ addition by FA has quenched the native fluorescence of NCD, and this FA-NCD was used as a fluorescence probe to detect Hcy. The incremental addition of Hcy to FA-NCD has triggered the turn-on response of

quenched fluorescence and facilitated the detection of Hcy with an LoD of 2.276 µM. The probe could be able to detect Hcy without interference by cysteine and glutathione, both were unable to turn -on the fluorescence of FA-NCD.

2. Materials and Methods

2.1 Materials

Citric acid, cholesterol, glucose, and urea were purchased from Merck Life Science Private Limited, India. Homocysteine, L- cysteine, glutathione, and L-methionine were purchased from Sigma Aldrich. Folic acid, histidine, tryptophan, and glycine were obtained from Merck SA, Darmstadt, Germany. Creatinine, uric acid, phenylalanine, and tyrosine from Spectrochem Pvt. Ltd., Mumbai, India. Ferric chloride hexahydrate, zinc chloride, and copper chloride were bought from Nice chemicals Pvt. Ltd. Kochi, Kerala, India. All experiments were done with double distilled water.

2.2.Instruments

The absorbance spectra were recorded with Horriba Scientific Duetta fluorescence and absorbance spectrometer. The ATR- FTIR spectral measurements of solid and liquid samples were done with Agilent Technologies' Cary 630 model FTIR spectrometer over 400-4000cm^{-1}. The DLS and Zeta measurements were done with a Horriba scientific SZ-100 nanoparticle Analyzer. The fluorescence spectra of liquid samples were recorded at room temperature using Jasco FP-750 spectrofluorometer made by Jasco, Japan. TCSPC analysis was done with the Edinburgh instrument's FLS1000 model instrument. HR-TEM analysis was done with a 200kV electron microscope model JEOL/JEM2100. The synthesis of carbon dots was done with a domestic microwave oven Panasonic NNSM255W model. Electron Spray Ionisation (ESI) Mass spectra were taken using Advion expression$^{L}{}_{CMS}$ model mass spectrometer.

3. Experimental methods

3.2.Synthesis of nitrogen-doped carbon dots (NCD)

As per prior reports, the synthesis of nitrogen-doped carbon dots (NCD)s was done with slight modification[22,23]. The precursors used for NCDs were citric acid as a carbon source and urea as a dopant of nitrogen source. Briefly, 3.0 g of citric acid and 3.0 g of urea were weighed and mixed well with 10mL double distilled water. The mixture was then microwave irradiated for about 90 seconds under 750 watts in a domestic microwave oven. The digital

photograph of as-synthesized NCD is shown in **Fig.S1**. A color change indicated the formation of NCDs from colorless to orange-brown color. The orange-brown colored syrupy liquid was collected, cooled down to room temperature, and dissolved in 20mL water. It was then dialyzed using a 12kDa dialysis membrane. The obtained NCDs exhibited bright green fluorescence under UV light of 365nm. The NCDs were stored in a refrigerator under four ºc.

3.3. Development of Folic acid conjugated NCD (FA-NCD)

The FA-NCDs were obtained by ex-situ method of incorporation using incremental addition of 0.1mM stock solution of FA. For this, 1mL of NCD was diluted with 20 mL of double-distilled water, and 3 mL each of this solution was taken in a beaker and added to different volumes of 0.1 M FA (0- 1000 µL) and stirred well for about 60 seconds in the dark at room temperature to get 0 - 16 µM FA-NCDs. The fluorescence properties of NCDs after ex-situ addition by FA were studied.

3.4.Fluorescence detection of homocysteine

3.0 mL of 2 µM FA-NCD was taken in a cuvette. A series of 50 µL volumes of the required concentration of Hcy was added, shaken well for about a minute, and a fluorescence emission scan was recorded at an excitation wavelength of 440 nm.

3.5. Real sample assay

The possibility of clinical application of the probe was investigated in a natural biological matrix. The urine and serum samples were collected from healthy individuals in the morning and were spiked with the required concentration of Hcy. The real sample analysis was carried out with concentrated serum and urine and also with their ten times diluted and 100 times diluted solutions. The real sample analysis was done in the same manner as that of Hcy detection in the aqueous medium.

3.6. Paper strip assay

The conceivable use of the developed probe to detect Hcy at the point of care was studied by devising a paper-based assay. Whatman 40 filter paper was cut into 1cm X 5cm dimensions and coated with 2 µM FA-NCD. Dried in the dark and onto this dried strip, Hcy was added.

4. Results and discussions

4.1 Synthesis and characterization of NCD and FA-NCD

The NCDs were prepared by a one-pot microwave-assisted method using citric acid and urea as the sources of carbon and nitrogen, respectively, as per previous reports[22,23]. The obtained NCDs exhibited bright green fluorescence under UV radiation of wavelength 365 nm. The photoluminescence (PL) properties were studied by recording emission scans with excitation wavelengths ranging from 260 to 480 nm, and the maximum emission was observed upon excitation at 440 nm (**Fig.1A**). The emission was observed in the range of 500 to 550 nm.

The NCDs were characterized using different analytical methods: FTIR, DLS, Zeta, and HR-TEM techniques. The FTIR spectra of NCD and its precursors were recorded and compared to get an insight into the surface functionalities present in NCD. The FTIR spectra of NCD and its precursors are shown in **Fig.1(B)**. The broadband at 3192 and 3420 cm^{-1}indicates N-H and O-H stretch correspondingly[24–27]. The band at 1769 cm^{-1} refers to C = O stretching of α, β unsaturated carboxylic acid functionalities present in cetirizine acid derivatives. The broad peak at 1650 cm^{-1} was attributed to N-H bending vibrations[28]. The UV-Vis absorption spectrum of NCD exhibited a characteristic absorption peak around 350 nm, shown in **Fig.S2(A).** The size distribution studies of NCDs by the dynamic light scattering method reported a hydrodynamic diameter of 9.5 nm, depicted in **Fig. 2(C)**. The zeta potential of NCD was shown in **Fig.S2(B)**, which was -3.7 mV, indicating the occurrence of negative charge moieties at the surface and the good dispersion of carbon quantum dots[29]. The morphological characterization of NCD was done with the HR-TEM technique and is represented in **Fig.2(A)**. The average size of NCD was found to be 5 nm. The SAED pattern of NCD shown in **Fig.2(B)** indicates the amorphous nature of the synthesized NCD[30,31]. The fluorescence decay profile of NCD was analyzed by the time-correlated single-photon counting (TCSPC) technique shown in **Fig.5(A)**. The NCD followed a single exponential decay pathway with an average lifetime of 6.725 ns.

4.2. Development of Folic acid incorporated NCDs (FA-NCD)

The ex-situ addition strategy was utilized to get FA-NCD. To the purified NCDs (3 mL) received after microwave synthesis, different volumes of 0.1 mM stock solution of FA were added and incubated for 60 seconds in the dark at room temperature to get 0 -16 µM FA-NCD. We observed the FA-inflicted quenching behavior at varying time intervals and optimized one-minute time as the optimum incubation time. This mainly helped to ensure proper mixing such that maximum FA molecules can interact with NCD to avoid variations in fluorescence measurements and get a stable fluorescence intensity. We kept one minute as the standard incubation time throughout the study to minimize errors and false positives. The fluorescence studies revealed that the fluorescence intensities of NCD were decreased upon incremental addition by FA. The fluorescence emission scans of NCDs upon the addition of 0 - 16 µM FA were depicted in **Fig.3(A)**. The native fluorescence of NCDs was quenched continuously with incremental addition by FA from 0 – 16 µM. It was observed that 2.67 µM FA was enough to quench the innate fluorescence of NCD to 73.84 %. The addition of FA has quenched the fluorescence intensity of NCD exponentially and is shown in **Fig.3(B)**. The linear Stern-Volmer plot depicting the quenching of fluorescence of NCD by ex-situ addition of 0 - 6 µM FA is swn **Fig. 3(C).** The linear response available be represented as $\left(\frac{I0}{I}\right) = 0.3349[FA] + 0.79103$ (with an R^2 of 0.9865) where [FA] is the concentration of folic acid in µM, I_0 is the fluorescence intensity of virgin NCD, and I is that of FA-NCD. The equation 3σ/k is used to obtain the limit of detection (LoD) of FA and was found to be 2.97 µM, where σ is the standard deviation and k is the slope of the linear plot.

The limit of quantification (LoQ) was calculated using the equation 10σ/k where σ and k are the standard deviation and slope of the linear plot, respectively, and was found to be 9.925 µM. The effect of pH upon quenching of fluorescence of NCD by 2.67 µM FA addition was studied and was shown in **Fig. S3**. The maximum quenching was observed at a pH of 5.5 and was selected for further studies. The decreased quenching efficiency at acidic pH may be attributed to the poor solubility of FA in an acidic medium[32]. The fluorescence decay profile of FA-NCD was depicted in **Fig.5(B).** It exhibited a single exponential decay pathway of 4.120 µs (99.92%). Since the ratio of average lifetime values of NCDs (6.725 ns) and FA-NCDs (4.498 µs) is more significant than unity rules out the static quenching mechanism between NCD and FA. The substantial change in fluorescence lifetime points to dynamic quenching as the plausible quenching mechanism manifests between the two systems[27,33].

The UV-Vis absorption spectra of NCD, FA-NCD, and pure FA were recorded and was shown in **Fig.S6**. The NCD has an absorption peak of around 340 nm which may be attributed to n to π* transition of the C=O or C=N bond[34] and folic acid has absorption peaks of around 370 nm and 275 nm which may be assigned to the π to π* transitions of p-amino benzoic acid and pterin ring moieties[35,36]. In the case of the NCD-FA, the peak of the studied NCD persists and an additional peak is present at around 275 nm which may be attributed to FA present in the system. The absence of new peaks other than that of pure FA also supports the possibility of a dynamic quenching mechanism between NCD and FA. Further, the quenching of fluorescence of NCD by FA was at different temperatures of 12, 40, and 56 ºC the fluorescence spectra of NCD-FA at these temperatures and the corresponding linear Stern- Volmer plots were shown in **Fig.S9**. It was observed that the slope of the linear plot was increased from temperature 12 to 56ºC which also points to the possibility of a dynamic quenching mechanism. With the possibility of an inner filter effect between NCD and FA by virtue of the strong absorption of FA, we recorded the UV-Vis absorption spectrum of pure FA (**Fig.S6 (A)**). The absorption and emission wavelength of FA and NCD and compared and consolidated in **Table S4**. Since there exists a mismatch between the absorption and emission wavelengths of NCD and FA, we can safely rule out the possibility of an inner filter effect in the probe.

4.3. Turn-on response of FA-NCD towards homocysteine

The fluorescence response of FA-NCDs towards the incremental addition of 10 µL Hcy was studied with a 0.1 mM stock solution of Hcy. The fluorescence enhancement was observed upon gradual addition of Hcy in the concentration ranging from 0-50 µM. The excitation wavelength of measurements was kept constant at 440 nm. A four-fold fluorescence enhancement was observed with an increasing concentration of Hcy. A red shift in fluorescence emission spectra of FA-NCD was observed upon the addition of Hcy. The surface state mechanism may be the reason behind the red shift of the fluorescence emission spectrum upon the addition of Hcy. Many studies suggest the direct involvement of surface states such as surface functional groups, the changes in surface oxidation, etc. in the fluorescence of carbon dots. The red shift in emission wavelengths of carbon dots may observe upon capturing the excited state energy by surface states. The oxygen-related groups may undergo surface oxidation, thereby creating a defect that is able to trap the excitons. The

radiations arising from the recombination of trapped excitons channelize the red-shifted emission due to the generation of numerous new lower energy levels. That is these defects may create more emission sites on the carbon dot surface, and these surface defects may trap more excitons causing a red shift in the emission spectrum[37,38]. The digital photographs of NCD, FA-NCD, and FA-NCD-Hcy in daylight and UV light are shown in **Fig. S4**. The fluorescence turn-on response of FA-NCD towards incremental addition of Hcy was depicted in **Fig.4(A).** A plot of I/I_0 against [Hcy] was studied where I_0 and I are the fluorescence intensities before and after the addition of Hcy, and a linear response was observed in the concentration range 0 - 50 µM exhibiting an LoD of 2.276 µM and LoQ of 9.425 µM. It is depicted in **Fig.4(B).** The fluorescence decay profile of FA-NCD in the presence of Hcy by TCSPC analysis revealed a biexponential decay pathway with 3.153 ns (35.09 %) and 7.814 ns (64.91 %) with an average lifetime of 6.178 ns {**Fig.5(C)**}.

4.4. Plausible mechanism

The plausible mechanism of sensing may arise from the specific interaction between FA and Hcy. From the fluorescence decay profile analysis of NCD, FA-NCD, and FA-NCD-Hcy (**Fig.5**), we can predict that a dynamic quenching mechanism is manifesting between the systems NCD and FA-NCD characterized by a notable change in the average lifetime. The UV-Vis absorption spectra and FT-IR data also support a dynamic quenching mechanism. The UV-Vis absorption spectra and FTIR spectra of NCD, FA-NCD, and FA-NCD- Hcy were taken in **Fig.S6** and **S7,** respectively. It has been identified that Hcy upon disulfide bond formation promotes reactive oxygen species and free radical generation [39]. As reported earlier, the two distinctive features of Hcy chemistry may be the reason underlying the selective response of the probe over other thiols such as cysteine. Viz, (1) The additional carbon atom in Hcy favors Hcy as a five-membered ring thiolactone[3,8,40]. This five-membered thio lactone may interact with the free NH_2 group of FA. (2) The kinetically favored Hydrogen Atom Transfer (HAT) reaction by Hcy thiyl radical provides an alpha - amino carbon-centered radical. When the amino group is uncharged, the ^{a}C-H bond is weaker than its S-H bond. The thiyl radical of Hcy can mediate a Hydrogen atom transfer (HAT) reaction that was kinetically favored to provide an alpha-amino carbon-centered radical. Since the five-membered ring transition state formed by Hcy is kinetically favored for HAT

reaction over other bio thiols[41–43]. In order to ascertain this fact, we conducted the Electron Spray Ionization (ESI) mass spectra of NCD and NCD in presence of FA and Hcy were taken and were shown in **Fig.S10 A and B** respectively. The peak at m/z 153.1 indicates the presence of homocysteine thiolactone which facilitate HAT. This points to the feasibility of these suggested mechanisms but much more studies in the future may be required to confirm the actual mechanism. HAT for Hcy was found to be effective in mildly acidic and neutral pH, and this may be the reason for the better performance of our sensor at this pH.[39].

4.5.Selectivity and interference studies.

The performance of the sensor towards the selective detection of Hcy was studied with several co-existing biomolecules, ions, and structural analogs of Hcy, including glutathione, cysteine, glucose, cholesterol, hemoglobin, creatinine, uric acid, histidine, tyrosine, methionine, tryptophan, phenylalanine glycine, etc. and ions such as Zn^{2+}, Cu^{2+}, $Fe^{3+,}$ etc. The response in the selectivity study was represented in **Fig.6(A)**. In this study, the concentration of the possible potentially interfering co-existing biomolecules/ions was kept at a thousand times higher than the concentration of Hcy, such that the concentration of these biomolecules /ions in solution was much greater than that in a normal healthy human and equal /higher to that in the diseased state reflected by the corresponding biomarker. Most of the co-existing biomolecules quenched the fluorescence of FA-NCD, while some others like glucose, methionine, tyrosine, and glycine gave only a marginal enhancement in fluorescence which does not cause much interference in the selective detection of Hcy. In the case of real sample analysis, an experienced clinician can cleverly impose his clinical wisdom to discrete this marginal effect. The most important observation we got was that the most potent interfering molecules, glutathione, and cysteine, could not turn on the fluorescence. Still, they further quenched the fluorescence of FA-NCD. Thus, our probe successfully circumvented the challenge of interference by cysteine and glutathione.

Similar results were observed in interference studies also. In interference studies, we checked the ability of the probe to detect Hcy in the presence of a single competing molecule/ion and the presence of a mixture of these biomolecules /ions. The results obtained were plotted in **Fig.6(B).** The probe exhibited appreciable selective detection of Hcy in the presence of single biomolecule/ions as well as their mixture. Considering the slight turn-on response of FA-NCD towards glucose which is an important co-existing potentially

interfering biomolecule in clinical diagnosis we have further studied the selectivity and interference of glucose at different elevated threshold concentration levels. For this, the concentration of glucose levels in normal (<7.8 mM), pre-diabetic (7.9 – 11.79 mM), diabetic (11.8 mM), and highly diabetic (>11.8 mM) conditions were selected and fluorescence responses were recorded. To these concentrations, a 5 μM of Hcy solution was added and again fluorescence response was noted. The observations were consolidated as a bar diagram shown in **Fig.S11**. It was observed that even in the presence of high glucose concentration the probe exhibited a turn-on response detecting Hcy without much interference.

4.6. Paper strip assay

The use of the probe for the onsite detection of Hcy by a paper-based point of care strip was attempted with a Whatman 40 filter paper. The Whatman 40 filter paper was coated with the probe and dried in the dark, and the Hcy was introduced at the surface of the probe. The digital photographs of developed paper strips are exhibited in **Fig.S8**. The developed paper strip exhibited an appreciable fluorescence turn-on response towards Hcy, indicating that the probe is a potential candidate for the point of care detection of Hcy.

4.7. Real sample analysis

To ensure the clinical utility of the proposed fluorescent probe in detecting Hcy, we checked the probe with actual biological samples. The analysis was conducted with spiked urine and serum samples and ten times and 100 times diluted samples. The results were tabulated in **Table S1 and Table S2,** respectively. The change in fluorescence intensities before and after adding Hcy in serum and urine samples at different dilutions was graphically shown in **Fig.S5**. A good recovery percentage in the range of 98- 103 % was obtained, confirming the applicability of the developed probe to detect Hcy in real matrices. A comparison of the efficiency of the proposed examination with other previously reported investigations was given in **Table S3**.

5. Conclusion

In a nutshell, we developed folic acid-incorporated nitrogen-doped carbon dots and were aimed at the selective fluorescence detection of Hcy. The designed fluorescence probe detected Hcy selectively without interference from cysteine and glutathione with a low LoD. A low-cost paper strip assay for detecting Hcy with the investigation was successfully developed. The performance of the FA-NCD for detecting Hcy was successfully validated

with a good recovery percentage in real urine and serum samples proposing its potential clinical utility.

Acknowledgment

The authors are thankful to the Head, Department of Chemistry, University of Kerala, Kariavattom, Thiruvananthapuram, the Director, CLIF, University of Kerala, and Director, STIC, CUSAT, Kochi for extended laboratory and instrumental facilities. Anju S. Madanan is thankful to the University of Kerala for financial support as a university junior research fellowship.

Ethical statement

The experiments were done by following the ethical standards of the Indian Council of Medical Research (ICMR). They were approved by the human ethical committee of the University of Kerala, Thiruvananthapuram.

Conflicts of interest

The authors declare no competing financial interest.

REFERENCES

[1] C. Yu, F. Zeng, M. Luo, S. Wu, A silica nanoparticle-based sensor for selective fluorescent detection of homocysteine via interaction differences between thiols and particle-surface-bound polymers, Nanotechnology. 23 (2012) 305503. https://doi.org/10.1088/0957-4484/23/30/305503.

[2] cardiovascular diseases (CVDs), (n.d.). https://www.who.int/en/news-room/fact-sheets/detail/cardiovascular-diseases-(cvds) (accessed August 26, 2021).

[3] W. Wang, J.O. Escobedo, C.M. Lawrence, R.M. Strongin, Direct Detection of Homocysteine, J Am Chem Soc. 126 (2004) 3400–3401. https://doi.org/10.1021/ja0318838.

[4] L. Yang, Y. Su, Y. Geng, Y. Zhang, X. Ren, L. He, X. Song, A Triple-Emission Fluorescent Probe for Discriminatory Detection of Cysteine/Homocysteine, Glutathione/Hydrogen Sulfide, and Thiophenol in Living Cells, ACS Sens. 3 (2018) 1863–1869. https://doi.org/10.1021/acssensors.8b00685.

[5] Q. He, R. Li, Z. Yuan, H. Kassaye, J. Zheng, C. Wei, F. Wang, Y. Yao, L. Gui, H. Chen, A turn-on near-infrared fluorescent probe for detection of cysteine over glutathione and homocysteine in vivo, Analytical Methods. 11 (2019) 1857–1867. https://doi.org/10.1039/c8ay02792g.

[6] L. Yang, Y. Su, Y. Geng, Y. Zhang, X. Ren, L. He, X. Song, A Triple-Emission Fluorescent Probe for Discriminatory Detection of Cysteine/Homocysteine, Glutathione/Hydrogen Sulfide, and Thiophenol in Living Cells, ACS Sens. 3 (2018) 1863–1869. https://doi.org/10.1021/acssensors.8b00685.

[7] H. Peng, K. Wang, C. Dai, S. Williamson, B. Wang, Redox-based selective fluorometric detection of homocysteine, Chemical Communications. 50 (2014) 13668–13671. https://doi.org/10.1039/c4cc03677h.

[8] Y. Zou, X. Feng, Y. Zhao, Z. Wei, W. Zhu, M. Zhao, T. Wang, Z. Liu, S. Tang, G. Wang, Q. Guo, D. Chen, Selective homocysteine detection of nitrogen-doped graphene quantum dots: Synergistic effect of surface catalysis and photoluminescence sensing, Synth Met. 267 (2020). https://doi.org/10.1016/j.synthmet.2020.116432.

[9] W. Wang, O. Rusin, X. Xu, K.K. Kim, J.O. Escobedo, S.O. Fakayode, K.A. Fletcher, M. Lowry, C.M. Schowalter, C.M. Lawrence, F.R. Fronczek, I.M. Warner, R.M. Strongin, Detection of homocysteine and cysteine, J Am Chem Soc. 127 (2005) 15949–15958. https://doi.org/10.1021/JA054962N/SUPPL_FILE/JA054962NSI20050919_011704.PDF.

[10] H. Refsum, A.D. Smith, P.M. Ueland, E. Nexo, R. Clarke, J. McPartlin, C. Johnston, F. Engbaek, J. Schneede, C. McPartlin, J.M. Scott, Facts and recommendations about total homocysteine determinations: an expert opinion, Clin. Chem. 50 (2004) 3–32. https://doi.org/10.1373/clinchem.2003.021634.

[11] O. Nekrassova, N.S. Lawrence, R.G. Compton, Analytical determination of homocysteine: a review, Talanta. 60 (2003) 1085–1095. https://doi.org/10.1016/s0039-9140(03)00173-5.

[12] J.O. Escobedo, W. Wang, R.M. Strongin, Use of a commercially available reagent for the selective detection of homocysteine in plasma, Nature Protocols 2006 1:6. 1 (2007) 2759–2762. https://doi.org/10.1038/nprot.2006.399.

[13] D. Rautiola, Detection of Homocysteine with Bridged Viologen Chemical Probes, Portland, OR, 2000. https://doi.org/10.15760/etd.1540.

[14] D.S. Wald, M. Law, J.K. Morris, Papers Homocysteine and cardiovascular disease: evidence on causality from a meta-analysis, n.d.

[15] H. Kobayashi, M. Ogawa, R. Alford, P.L. Choyke, Y. Urano, New Strategies for Fluorescent Probe Design in Medical Diagnostic Imaging, (2009). https://doi.org/10.1021/CR900263J.

[16] H. Liu, Y. Sun, J. Yang, Y. Hu, R. Yang, Z. Li, L. Qu, Y. Lin, High performance fluorescence biosensing of cysteine in human serum with superior specificity based on

carbon dots and cobalt-derived recognition, Sens Actuators B Chem. 280 (2019) 62–68. https://doi.org/10.1016/j.snb.2018.10.029.

[17] K. Wang, Z. Tang, C.J. Yang, Y. Kim, X. Fang, W. Li, Y. Wu, C.D. Medley, Z. Cao, J. Li, P. Colon, H. Lin, W. Tan, Molecular engineering of DNA: Molecular beacons, Angewandte Chemie - International Edition. 48 (2009) 856–870. https://doi.org/10.1002/ANIE.200800370.

[18] Z.Q. Liu, Y.Q. Huang, W.Y. Sun, Progress in fluorescent recognition and sensing of solvent and small organic molecules based on metal-organic frameworks, Chinese Journal of Inorganic Chemistry. 33 (2017) 1959–1969. https://doi.org/10.11862/CJIC.2017.244.

[19] N.A. Humaera, A.N. Fahri, B. Armynah, D. Tahir, Natural source of carbon dots from part of a plant and its applications: a review, Luminescence. 36 (2021) 1354–1364. https://doi.org/10.1002/BIO.4084.

[20] J. Wang, Y. Liu, M. Jiang, Y. Li, L. Xia, P. Wu, Aldehyde-functionalized metal-organic frameworks for selective sensing of homocysteine over Cys, GSH and other natural amino acids, Chemical Communications. 54 (2018) 1004–1007. https://doi.org/10.1039/c7cc08414e.

[21] Y. Zou, X. Feng, Y. Zhao, Z. Wei, W. Zhu, M. Zhao, T. Wang, Z. Liu, S. Tang, G. Wang, Q. Guo, D. Chen, Selective homocysteine detection of nitrogen-doped graphene quantum dots: Synergistic effect of surface catalysis and photoluminescence sensing, Synth Met. 267 (2020). https://doi.org/10.1016/j.synthmet.2020.116432.

[22] J.S.A. Devi, R.S. Aparna, B. Aswathy, J. Nebu, A.O. Aswathy, S. George, Understanding the Citric Acid–Urea Co–Directed Microwave Assisted Synthesis and Ferric Ion Modulation of Fluorescent Nitrogen Doped Carbon Dots: A Turn On Assay for Ascorbic Acid, ChemistrySelect. 4 (2019) 816–824. https://doi.org/10.1002/slct.201803726.

[23] S. Qu, X. Wang, Q. Lu, X. Liu, L. Wang, S. Qu, Q. Lu, X. Liu, L. Wang, X. Wang, Carbon Nanodots A Biocompatible Fluorescent Ink Based on Water-Soluble Luminescent Carbon Nanodots**, Angew. Chem. Int. Ed. 51 (2012) 12215–12218. https://doi.org/10.1002/anie.201206791.

[24] X. Zhao, J. Zhang, L. Shi, M. Xian, C. Dong, S. Shuang, Folic acid-conjugated carbon dots as green fluorescent probes based on cellular targeting imaging for recognizing cancer cells, RSC Adv. 7 (2017) 42159–42167. https://doi.org/10.1039/c7ra07002k.

[25] S.K. Bhunia, A.R. Maity, S. Nandi, D. Stepensky, R. Jelinek, Imaging Cancer Cells Expressing the Folate Receptor with Carbon Dots Produced from Folic Acid, ChemBioChem. 17 (2016) 614–619. https://doi.org/10.1002/cbic.201500694.

[26] L. Shi, D. Chang, G. Zhang, C. Zhang, Y. Zhang, C. Dong, L. Chu, S. Shuang, Co2+ detection, cell imaging, and temperature sensing based on excitation-independent green-fluorescent N-doped carbon dots, RSC Adv. 9 (2019) 41361–41367. https://doi.org/10.1039/c9ra09405a.

[27] R.R. Anjana, J.S. Anjali Devi, M. Jayasree, R.S. Aparna, B. Aswathy, G.L. Praveen, G.M. Lekha, G. Sony, S,N-doped carbon dots as a fluorescent probe for bilirubin, Microchimica Acta. 185 (2018). https://doi.org/10.1007/s00604-017-2574-8.

[28] J. Nebu, K.S. Anu, J.S. Anjali Devi, R.S. Aparna, A.O. Aswathy, G.M. Lekha, G. Sony, Pottasium triiodide enhanced turn-off sensing of tyrosine in carbon dot platform, Microchemical Journal. 146 (2019) 12–19. https://doi.org/10.1016/j.microc.2018.12.021.

[29] T. Pal, S. Mohiyuddin, G. Packirisamy, Facile and Green Synthesis of Multicolor Fluorescence Carbon Dots from Curcumin: In Vitro and in Vivo Bioimaging and Other Applications, ACS Omega. 3 (2018) 831–843. https://doi.org/10.1021/acsomega.7b01323.

[30] Y. Zhang, L. Li, J. Yue, L. Cao, P. Liu, W.F. Dong, G. Liu, Yttrium-mediated red fluorescent carbon dots for sensitive and selective detection of calcium ions, Luminescence. 36 (2021) 1969–1976. https://doi.org/10.1002/BIO.4132.

[31] Q. Wang, Z. Zhang, T. Yang, Y. Han, Y. Cheng, J. Wu, J. Bai, C. Ma, Y. Niu, S. Shuang, Multiple fluorescence quenching effects mediated fluorescent sensing of captopril Based on amino Acids-Derivative carbon nanodots, Spectrochim Acta A Mol Biomol Spectrosc. 269 (2022) 120742. https://doi.org/10.1016/J.SAA.2021.120742.

[32] W. Li, X. Zhang, C. Miao, R. Li, Y. Ji, Fluorescent paper–based sensor based on carbon dots for detection of folic acid, Anal Bioanal Chem. 412 (2020) 2805–2813. https://doi.org/10.1007/s00216-020-02507-w.

[33] J.S. Anjali Devi, R.S. Aparna, R.R. Anjana, J. Nebu, S.M. Anju, S. George, Solvent Effects: A Signature of J- And H-Aggregate of Carbon Nanodots in Polar Solvents, Journal of Physical Chemistry A. (2019). https://doi.org/10.1021/acs.jpca.9b04568.

[34] P. Wu, W. Li, Q. Wu, Y. Liu, S. Liu, Hydrothermal synthesis of nitrogen-doped carbon quantum dots from microcrystalline cellulose for the detection of Fe3+ ions in an acidic environment, RSC Adv. 7 (2017) 44144–44153. https://doi.org/10.1039/C7RA08400E.

[35] F. Olmo, A. Rodriguez, A. Colina, A. Heras, UV/Vis absorption spectroelectrochemistry of folic acid, Journal of Solid State Electrochemistry. 26 (2022) 29–37. https://doi.org/10.1007/S10008-021-05026-5/FIGURES/3.

[36] Method development and validation of folic acid by UV-visible spectroscopy | international journal of pharmaceutical sciences and research, (n.d.). https://ijpsr.com/bft-article/method-development-and-validation-of-folic-acid-by-uv-visible-spectroscopy/ (accessed September 3, 2022).

[37] M. Liu, Optical Properties of Carbon Dots: A Review, Nanoarchitectonics. 1 (2020) 1–12. https://doi.org/10.37256/nat.112020124.1-12.

[38] A. Saengsrichan, C. Saikate, P. Silasana, P. Khemthong, W. Wanmolee, J. Phanthasri, S. Youngjan, P. Posoknistakul, S. Ratchahat, N. Laosiripojana, K.C.W. Wu, C. Sakdaronnarong, The Role of N and S Doping on Photoluminescent Characteristics of

Carbon Dots from Palm Bunches for Fluorimetric Sensing of Fe3+ Ion, Int J Mol Sci. 23 (2022). https://doi.org/10.3390/ijms23095001.

[39] M. Sibrian-Vazquez, J.O. Escobedo, S. Lim, G.K. Samoei, R.M. Strongin, Homocystamides promote free-radical and oxidative damage to proteins, Proc Natl Acad Sci U S A. 107 (2010) 551–554. https://doi.org/10.1073/pnas.0909737107.

[40] R. Zhao, J. Lind, G. Merényi, T.E. Eriksen, Kinetics of one-electron oxidation of thiols and hydrogen abstraction by thiyl radicals from α-amino C-H bonds, J Am Chem Soc. 116 (1994) 12010–12015. https://doi.org/10.1021/JA00105A048/ASSET/JA00105A048.FP.PNG_V03.

[41] E.L.R. Stokstad, S.W. Thenen, CHEMICAL AND BIOCHEMICAL REACTIONS OF FOLIC ACID, in: Analytical Microbiology, Elsevier, 1972: pp. 387–408. https://doi.org/10.1016/b978-0-12-403502-7.50042-9.

[42] M.M. Ic H A E L L U B R A N, The Biochemistry o f Folic Acid and Vitamin B12, 1971.

[43] C. Lu, Y. Zu, Specific detection of cysteine and homocysteine: Recognizing one-methylene difference using fluorosurfactant-capped gold nanoparticles, Chemical Communications. (2007) 3871–3873. https://doi.org/10.1039/b708603b.

****

Folic acid incorporated Nitrogen-doped Carbon dots as a turn-on fluorescence probe for homocysteine detection.

Anju S Madanan[a], Aswathy A.O. [a], Susan Varghese[a], Merin K. Abraham[a], Lekshmi R.S. [a], Ali Ibrahim Shkhair[a], Lekha G.M. [a], Syamchand S, S [b], and Sony George[a]

List of Figures

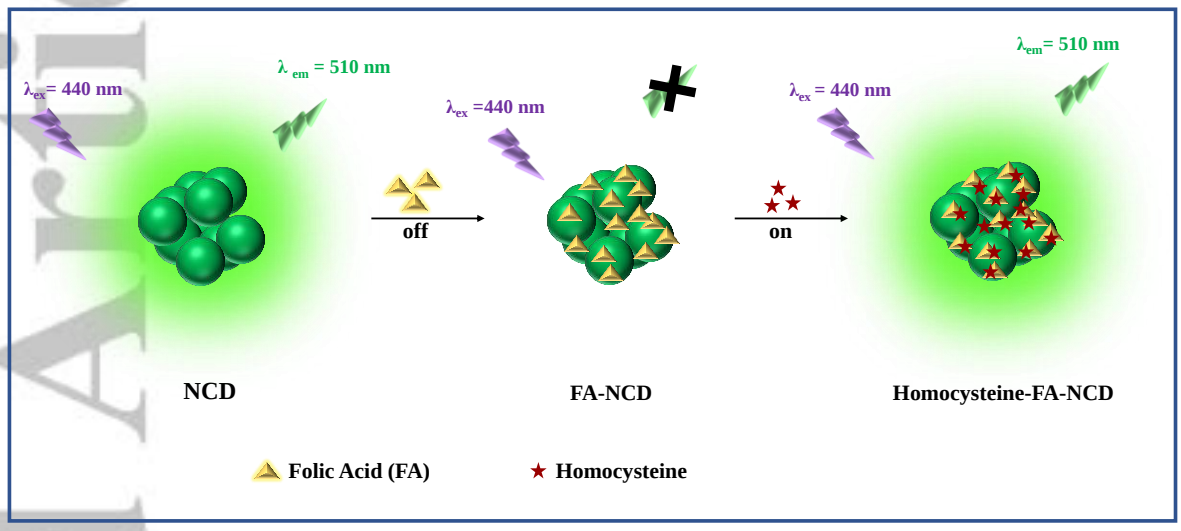

Scheme 1. Schematic representation of Fluorescence response of FA-NCD towards homocysteine.

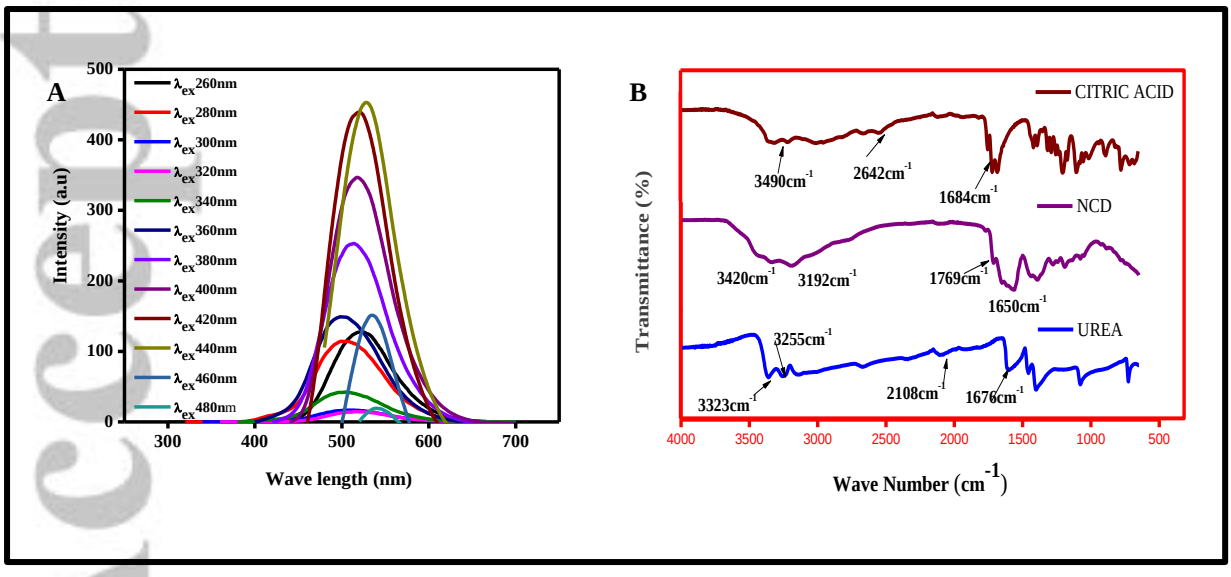

Fig.1. (A)The fluorescence emission spectra of NCD upon different excitation wavelength (260-480 nm) (B) FTIR spectra of NCD and its precursors citric acid and urea.

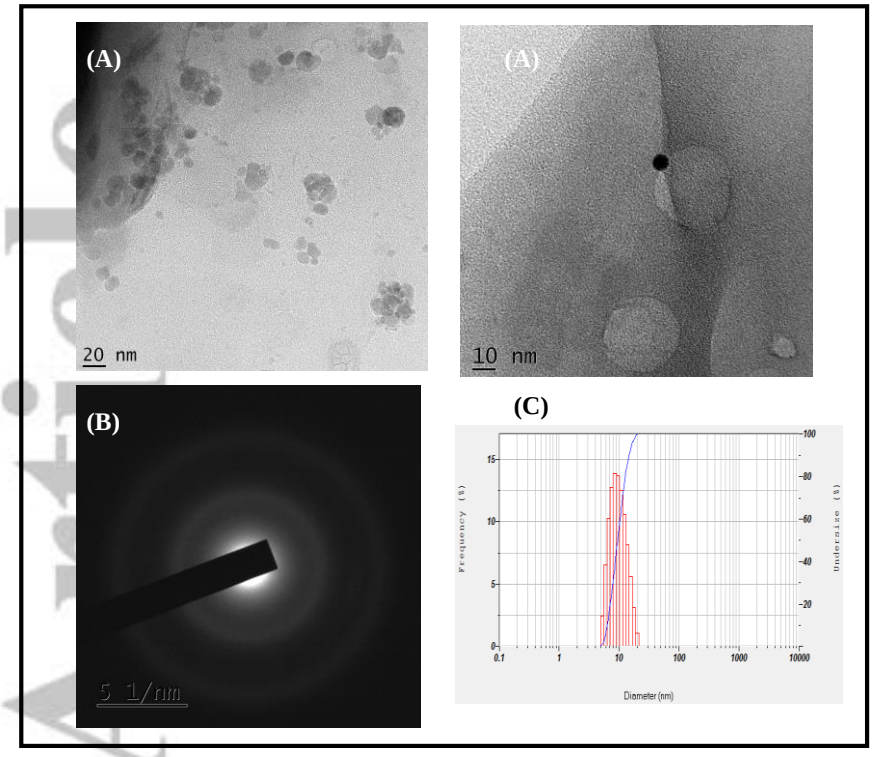

Fig.2. (A) HR-TEM images of NCD at 20 nm and 10 nm scales. (B) SAED pattern of NCD and (C) The DLS size distribution profile of NCD.

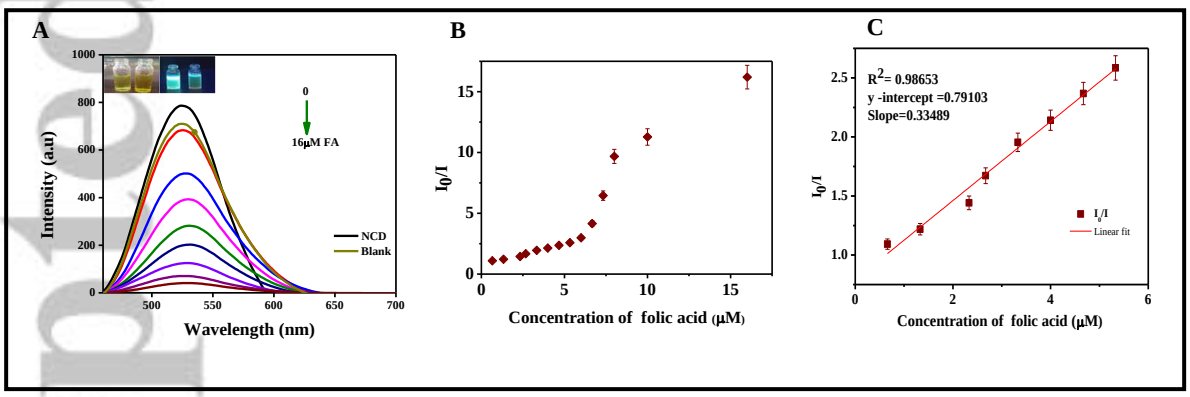

Fig.3. A) Fluorescence spectra of NCD upon addition of 0-16 μM FA solution (λ_{ex} = 440 nm). Digital Photographs of NCD and FA added NCD in daylight and UV light (Inset). **B)** The relative fluorescence intensities of NCD against the concentration of FA (λ_{ex} = 440 nm). (The I_0 and I are the fluorescence intensities of NCD before and after the addition of FA). **C)** The I_0 / I linear plot of the FA-NCD system (λ_{ex} = 440 nm). (The I_0 and I are the fluorescence intensities of NCD before and after the addition of FA).

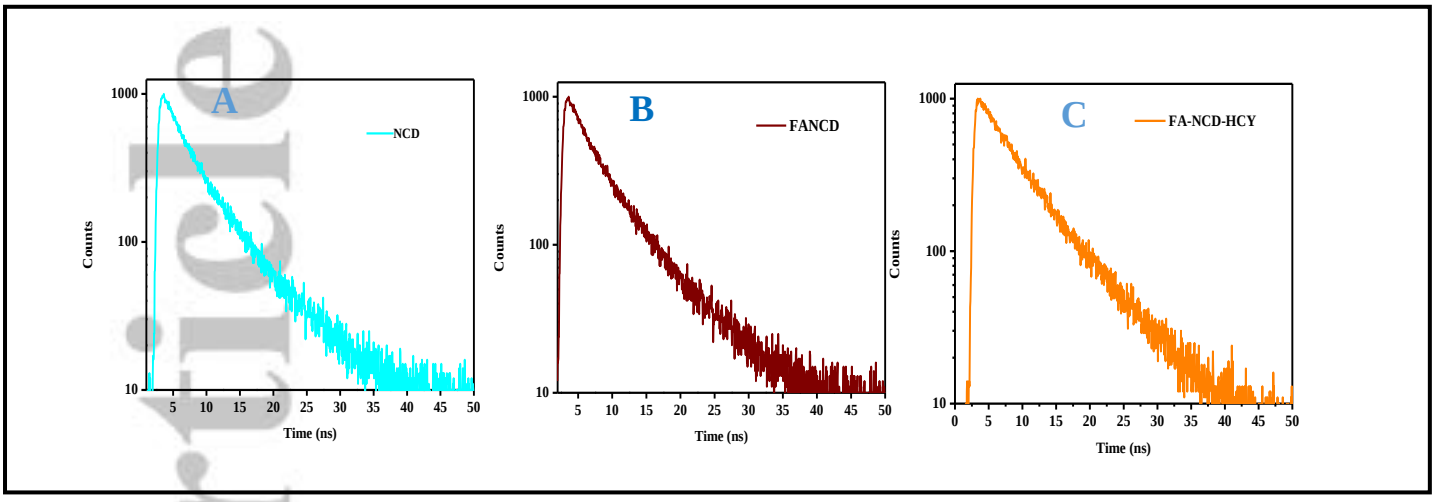

Fig.5. The fluorescence decay profile by TCSPC analysis of A) NCD B) FA- NCD C) FA-NCD-Hcy.

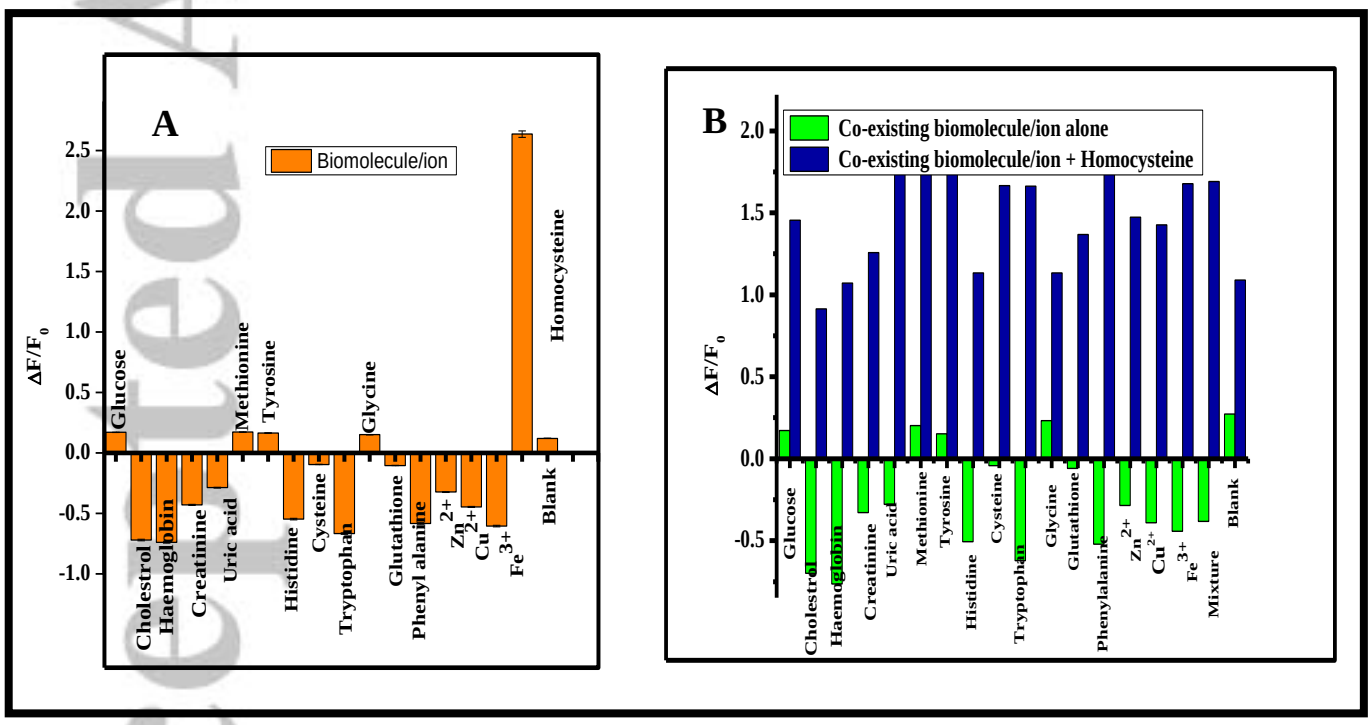

Fig.6. Bar diagram depicting the **A)** selectivity of FA-NCD towards Hcy in presence of other co-existing biomolecules/ions. **B)** interference study of FA-NCD towards Hcy in presence of other co-existing biomolecules/ions. [The concentration of the possible potentially interfering co-existing biomolecules/ions was kept at a thousand times higher than the concentration of Hcy,]